Deglaciation-Induced Climate Variability: An Explicit Model of the Glacial-Interglacial Transition That Simulates both the Bølling/Allerød and Younger-Dryas Events

By K. Sakai

Institute for Hydrospheric and Atmospheric Sciences, Nagoya University, Nagoya, Japan

W.R. Peltier

Department of Physics, University of Toronto, Toronto, Canada

(Manuscript received 20 February 1998, in revised form 5 October 1998)

Abstract

A previously developed two-dimensional-basin model of the global thermohaline circulation has been asynchronously coupled to an atmospheric energy balance model in support of analyses of the low frequency variability of the climate system. The coupled model, which has previously delivered successful simulations of the Dansgaard-Oeschger oscillations revealed in deep ice-core isotopic data from Summit, Greenland, is herein applied to the last deglaciation event of the current ice age in order to investigate the response of the climate system to transient meltwater forcing. The model employs hydrological forcing functions that consist of two components, one that is related to sea level and constrained by coral-based records of LGM to present sea level history, and a second that is unrelated to sea level and is assumed to exist because of the existence of the continental ice sheets that bounded the region of the North Atlantic basin where deep water is today. Our results show that the model successfully explains the occurrence of a Younger-Dryas-like cool period regardless of the detailed properties of the sea level-related meltwater event that is observed to have followed this millennium-long return to glacial conditions. In order to successfully explain the occurrence of the Bølling/Allerød warm period that occurred prior to the Y-D, however, the model requires the action of the additional "background" anomaly that is unrelated to sea level. We explore the impact on climate response of the properties of these two components of the anomalous forcing.

1. Introduction

It is now well-established that the rapid deglaciation process that followed the last glacial maximum (LGM, considered to correspond to 21 kyrBP = 21,000 sidereal years before present) of the current ice age and which transformed the climate of the ice-age Earth into its present Holocene state was interrupted by a cool period that is referred to as the Younger-Dryas (Y-D). Perhaps the most highly resolved records of North Atlantic sector climate history during the last deglaciation, including the Y-D period, consist of ice-core derived oxygen isotopic data from Summit, Greenland. These records constitute a primary output from the GRIP (GReenland Ice-core Project; *e.g.*, GRIP, 1993) and GISP2 (Greenland Ice-Sheet Project 2; *e.g.*, GISP2, 1993) collaborations. Such oxygen isotope records are a primary proxy for air temperature over the ice-sheet and these data suggest that temperature dropped during the Y-D to values as low as those obtained during full glacial conditions, with the amplitude of the temperature excursion reaching half that of the full glacial-interglacial change itself. The influence has been observed even far from the North Atlantic in mid-latitude, deep-sea cores from the Eastern Pacific (Kennett and Ingram, 1995).

Just prior to the Y-D, the proxy temperature record from Greenland shows that the climate in this sector was much closer to modern than to full glacial.

Corresponding author: K. Sakai, Inst. for Hydrospheric and Atmospheric Sciences, Nagoya University, Furocho, Chikusa-ku, Nagoya, Japan. E-mail: kotaro@ihas.nagoya-u.ac.jp
Present affiriation: Frontier Research System for Global Change, Seavans N., 1-2-1 Shibaura, Minato-ku, Tokyo, Japan 105-6791

At LGM, average surface temperature was of course the lowest realized during the ice age cycle. Thus, there exists a sharp transition in the climate record from LGM conditions to the warm period that preceded the onset of the Y-D. This warm period is referred to as the Bølling/Allerød (B/A), and according to the Summit isotopic data it began at approximately 15 kyrBP and lasted until the onset of the Y-D, near 13 kyrBP. Although this B/A warm period may appear to exhibit a gradual cooling within, the most salient aspect of this precursor to the Y-D is that the warming that commenced with the onset of deglaciation at LGM occurred very slowly until the very abrupt onset of the Bølling/Allerød.

Figure 1 illustrates this sequence of events based upon a superposition of four different data sets: the GRIP oxygen isotopic record (Dansgaard *et al.*, 1993; Taylor *et al.*,1993), the GISP2 oxygen isotopic record (Grootes *et al.*, 1993; Meese *et al.*, 1994) as temperature records of the region, a Vostok (Antarctica) temperature record (Jouzel *et al.*, 1987), and the record of sea level change at Barbados (Fairbanks, 1990). Concerning the coral-based records of sea level change since the last glacial maximum, it is not only the record from Barbados (Fairbanks, 1989, Bard *et al.*, 1990), but also those more recently obtained from the Huon Peninsula of Papua New Guinea (Edwards *et al.*, 1993), and from Tahiti (Bard *et al.*, 1996), that support the existence of two-episodes of rapid deglaciation interrupted by the Y-D cool period.

Our purpose in this paper will be to focus upon these two questions, namely possible mechanisms underlying the occurrence and abrupt onset of the B/A warm period. For the purpose of the analyses we shall present, the same reduced model of low frequency climate system variability will be employed as that recently described in detail in Sakai and Peltier (1997). As we will demonstrate, the results of these analyses do appear to provide explanations both as to why the B/A warm period occurred and why it onset as abrupt as is recorded in the paleoclimate record. Our results for this event will be shown to compare very favorably with the ice-core derived temperature record from Greenland.

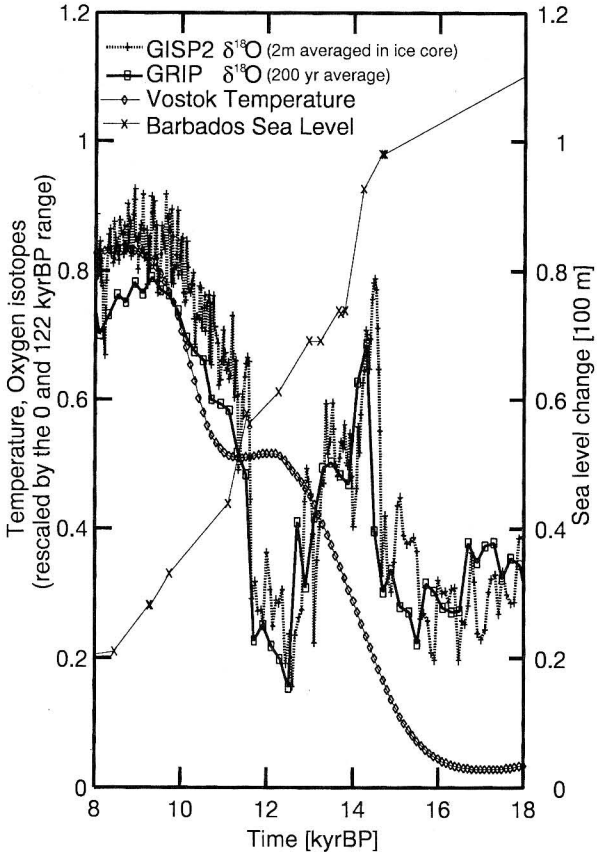

Fig. 1. Proxy records of climate variability between 8 kyr BP and 18 kyr BP. The Greenland temperature proxies, *i.e.*, oxygen isotope records from the GRIP and GISP2 deep ice cores are normalized by their maximum deviation between 0 and 122 kyr BP. The temperature record from Vostok, Antarctica is also normalized by its range between 0 and 122 kyr BP. See the original references referred to in the text for details.

2. Model overview

The climate model to be employed in this paper is essentially identical to that developed and employed in the context of our most recent discussion of Dansgaard-Oeschger oscillations (Sakai and Peltier, 1997). It originally consists of three primary components: a cryospheric component that describes the accumulation and flow of land ice stimulated by orbital insolation variations that will not be directly invoked in the present work; an atmospheric component consisting of a one-layer energy-balance model (EBM) that includes nonlinear seasonal ice (snow)-albedo feedback in the presence of orbital forcing; and finally an oceanic component that consists of two-dimensional (the vertical and one horizontal dimensions) coupled hydrodynamic slab representations of the major ocean basins.

The first two components of this model have been developed for the purpose of simulating the 100 kyr ice-age cycle itself. Detailed descriptions and applications of these elements of the coupled structure will be found, for example, in Deblonde and Peltier (1993) and references cited therein. Tarasov and Peltier (1997) have recently described the first fully successful application of this structure to the explanation of the 100 kyr cycle. The main prognostic variable of the atmospheric EBM is the surface temperature field, which is controlled by space-time variations of surface albedo (the default spatial distribution of the surface albedo may be determined

by seasonal snow cover, seasonal sea ice extent, or ice-sheet cover), topography, insolation, and additional forcing associated with variations in the concentration of greenhouse gases. Horizontal energy transport in the EBM is represented diffusively with a diffusion coefficient selected so as to enable the model to fit the observed latitudinal temperature variation in the modern system. The model contains neither an explicit hydrological cycle nor, of course, explicit fluid dynamics.

The final component of the model, and the one most important for the present application, is the oceanic component that was first coupled to the climate model in the analyses of Sakai and Peltier (1997) in order to investigate the role of the oceans on very long timescales (millennia). This element of the model began life as a stand-alone module, the initial formulation of which, along with paleoceanographic applications, was described in Sakai and Peltier (1995). In Sakai and Peltier (1996), this single-basin version of the model was extended to a multi-basin configuration and further paleoceanographic experiments described. Each of the four model basins in this extended model is two-dimensional, and three are meridionally oriented, *i.e.*, the Atlantic, Indian, Pacific; the Southern Ocean through which these three meridionally oriented basins are connected is oriented zonally. The velocity field in each of the model basins consists of two components, one of which is governed by a vorticity equation in which viscous dissipation of vorticity is balanced by density forcing, while the other derives from a parameterization of the wind-driven circulation.

The only interaction between the atmospheric and oceanic components of the model that is explicitly incorporated is a thermal interaction: the EBM determines the sea surface air temperature (SSAT) provided oceanic heat flux is known, and the oceanic component returns oceanic heat flux, provided SSAT is known. Since the atmospheric EBM does not have an internal hydrological cycle, the sea surface freshwater flux required by the ocean component of the model is externally specified. The overall structure of this field is fixed to that at present (annually averaged) forcing, a form perturbed so as to mimic the influence of freshwater runoff from the continents due to ice-sheet disintegration, which may or may not influence sea level depending upon the relationship of the magnitude of ablation to that of accumulation. The surface wind-stress that is required to drive the parameterized wind-driven circulation is fixed to the present annually averaged zonal wind stress. More detailed discussion of these boundary conditions and of the coupling scheme employed to link the individual model components is found in Sakai and Peltier (1996, 1997).

3. Deglaciation experiments: Hydrological perturbations

In Sakai and Peltier (1997), we assumed that the surface of the North Atlantic continuously received considerable anomalous freshwater forcing during the glacial epoch due to surface runoff (iceberg calving) from the large ice-sheets that covered North America and Northwestern Europe, a forcing that has the effect of reducing the surface salinity at high-latitudes. This hypothesis was based upon the sea surface salinity reconstruction for LGM by Duplessy *et al.* (1991) which clearly shows a sharp diminution of sea surface salinity (SSS). In all that follows we will continue to explore the implication of this scenario. It is important to understand that even if ice-sheet volumes were constant (so that sea level was also constant) we would still expect this hydrological perturbation to have been non-zero and equal in magnitude to the fraction of the precipitation falling on the ice-sheets that drained into the North Atlantic basin. In the work of Sakai and Peltier (1997), this first component of the anomalous flux was assumed to be constant in order to simplify interpretation of the results of the simulations concerning the mechanism underlying the D-O oscillations. Since continental ice-sheet extent decreases to zero during deglaciation, the magnitude of this component of the anomalous flux (which is unrelated to sea level) will certainly not be constant during this period but rather will also decrease to zero. It seems reasonable to assume, in a first approximation, that this background flux might have been proportional to the extent in continental ice cover. In what follows we will refer to this contribution to freshwater forcing as the North Atlantic *background anomaly* in order to distinguish it from the additional element of the forcing that is associated with a change in mean sea level. Detail of such a hydrological cycle, however, is beyond the purpose of this paper. We will instead investigate the model climate system through sensitivity experiments under various scenarios of anomalous freshwater forcing.

Figure 2 illustrates the assumed history of total anomalous freshwater forcing, to which we shall hereafter refer as the default deglaciation history. With the exception of two caveats, this deglaciation history has a sea-level related element that is identical to that employed in Sakai and Peltier (1996), which is constrained to fit the ICE-4G history of Peltier (1994, 1996). The first caveat is that 25 percent of the (sea-level related) first meltwater pulse from the Laurentide ice-sheet is assumed to flow through the Mississippi outlet while the remainder is assumed to flow through the St. Lawrence River outlet (in Sakai and Peltier (1996). All of the Laurentide ice-sheet derived meltwater was assumed to be discharged through the St. Lawrence

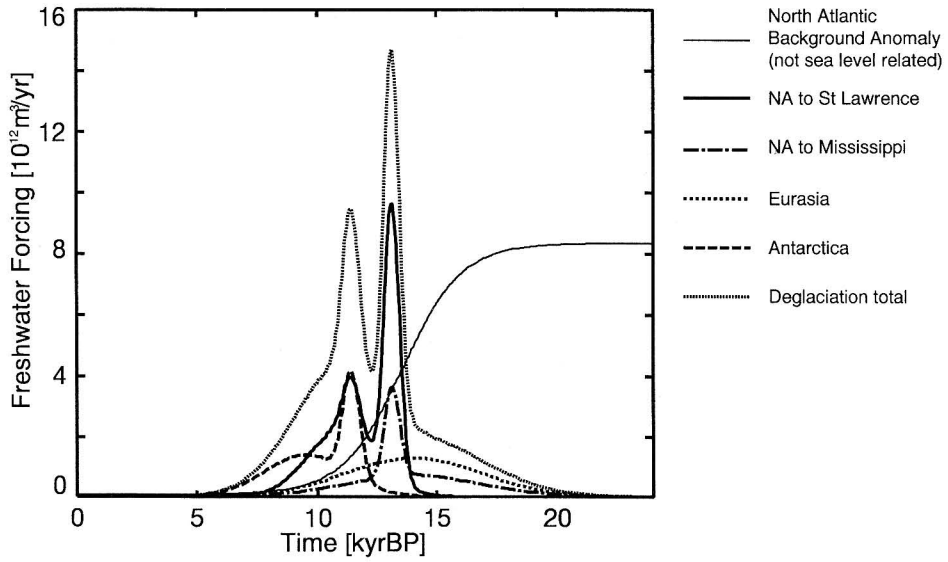

Fig. 2. Model of the components of anomalous freshwater loading applied to the oceanic component of the climate model. The thin solid line represents the background freshwater flux anomaly due to the existence of large continental ice sheets over North America and Europe which is unrelated to the changing sea level. The remaining curves represents the component of the anomalous flux that is directly connected to changing sea level and this is disaggregated into the contributions from various geographical regions. This component is based upon the results described in Fairbanks (1989) and Peltier (1994).

outlet). Because the ocean model is two dimensional, its response to an applied freshwater anomaly turned out to be insensitive to the latitude at which the anomaly is applied under the employed deglaciation meltwater history, and we will not comment further on this property of our experiments. The second caveat concerns the component of the anomalous forcing that was referred to as the *background anomaly*. This is the component of the anomalous forcing that is assumed to be *persistently* provided from the continental ice-sheets surrounding the high-latitude regions of the North Atlantic even when ice volume, and thus sea level, is constant. This contribution to the total anomalous forcing was discussed previously and, as we will see, it plays a crucial role in our ability to explain the rapid onset of the B/A warm period.

Based upon this default representation of the anomalous freshwater forcing, the results from three different series of sensitivity experiments will be presented in the following section of this paper. The first two series concern the sensitivity of the climate model to the amplitude and timing of the background anomaly (unrelated to sea level), whereas the final set of sensitivity experiments addresses the influence upon the variation of surface temperature due to the change of continental ice cover that occurs as deglaciation proceeds.

Figure 3 shows the model deglaciation histories to be employed in the first set of sensitivity experiments. In this series, only the initial amplitude of the background anomaly (hereafter referred as IBA) is varied, whereas the contributions from deglaciation related meltwater are held fixed to those of the default history shown on Fig. 2. The purpose of this

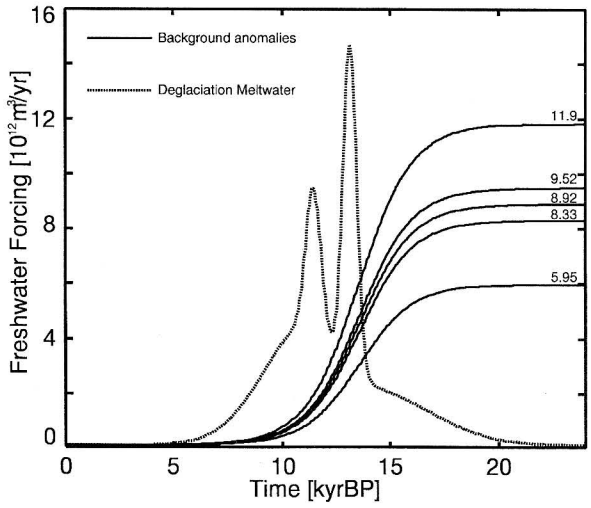

Fig. 3. Model deglaciation histories in terms of meltwater flux in the interval between 0 and 24 kyr BP for the first set of deglaciation experiments. In this set of experiments the sea level related contribution to the meltwater flux is fixed to the default history but the amplitude of the initial background anomaly is varied.

series of sensitivity experiments is to determine the magnitude of the IBA (if any) required to cause an abrupt warming sometime prior to the Y-D cold period that would enable us to accurately model the B/A warm period. This set of experiments is hereafter referred to as exp. I.

Figure 4 presents the model deglaciation histories to be employed in the second set of sensitivity experiments. In this sequence, the contributions from deglaciation-related meltwater are held fixed to those of the default history on Fig. 2. The IBA is also held fixed in amplitude but in this set of experiments the timing of the applied background anomaly is varied. The curve labeled "std" on the figure corresponds to the timing of the default deglaciation history. This set of experiments is clearly complementary to the first, and will enable us to examine the sensitivity of the systems' response to changes induced by the timing of the background anomaly. This set of experiments is hereafter referred as exp. II. An additional experiment is briefly described in the Appendix, in which we investigate the magnitude of the contribution to the temperature variation from the presence of the ice sheets themselves.

Throughout this series of experiments, the contributions to deglaciation-related meltwater production from Eurasia and Antarctica will be held fixed. Table 1 provides a summary of the experiments, which are to be discussed in what follows. In all of these experiments, the ocean component of the climate model is initialized in the state of strong pole-to-pole overturning that is characteristic of the modern circulation. Under the application of a small constant IBA, the thermohaline circulation in the Atlantic basin of the model converges to a new quasi-steady state within a few centuries of integration. Even under the considerably larger IBA applied herein, the model settles down to a new statistically steady state in less than a thousand years. All the experiments presented herein comprise integrations initialized at 24 kyrBP and terminated at 0 kyrBP, and include the full impact of the Milankovitch forcing over this time period.

4. Results and discussion

In this section we will discuss in sequence the result obtained in exp. I–II. Additional results and discussions on a further experiment (III), in which we will present the results obtained through experiments that incorporate the combined impact of freshwater flux induced changes in the strength of the THC and surface albedo variations associated with the changing surface area of the continental ice sheets, is presented in the Appendix.

4.1 Amplitude of the background freshwater flux anomaly: exp. I

In this set of experiments, the influence of the

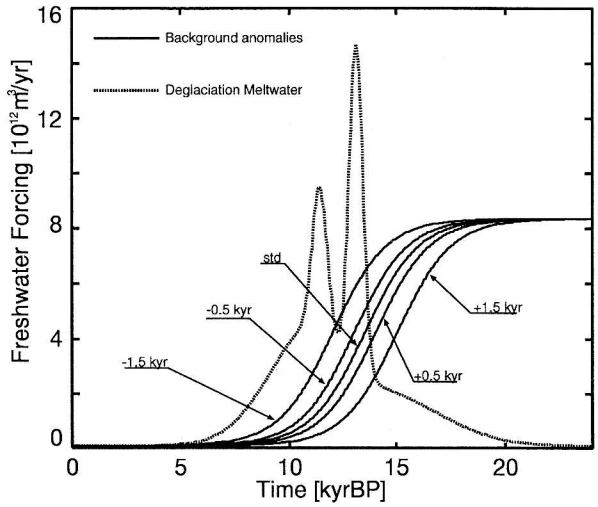

Fig. 4. Model deglaciation histories in terms of meltwater flux in the interval between 0 and 24 kyr BP for the second set of deglaciation experiments. In this set of experiments the sea level related contribution to the meltwater flux is held constant but the timing of reduction of the background anomaly is varied.

changes in the magnitude of the applied background anomaly is investigated as previously discussed. In Fig. 5 we plot the simulated meridional heat transport in the Atlantic basin of the model (difference between at 80°N and at 30°N). These time series reflect the intensity of NADW formation. The more intense the NADW formation, the larger the magnitude of the northward heat transport (due to choice of the coordinate system, northward heat transport is shown as a negative value).

In this Figure, data from 6 different cases is shown from the time interval between 20 kyrBP and 4 kyrBP. Without any background anomaly, which is the case presented on the top plate of Fig. 5, NADW formation is suppressed only during an overly brief *Y-D* period. Although this result appears to be very similar to the result obtained in the Y-D experiment described in Sakai and Peltier (1996), it should be noted that the duration of the model Y-D period obtained herein is significantly shorter than that produced in the previous analysis in which only the ocean component of the climate model was employed under a prescribed annual cycle of temperature. In the present experiment, the ocean component of the model is fully coupled to an atmospheric EBM that self-consistently determines SSAT and this coupling is important to the details of the Y-D event that the model simulates. The physical effect that reduces the duration of the low-NADW production state is therefore the negative feedback between the atmosphere and the ocean. The low-NADW production state that develops near 13 kyrBP is caused by

Table 1. List of deglaciation experiments

Experiment	description and notes
I	The response to variations of the amplitude of the initial background anomaly in freshwater flux applied to the North Atlantic is investigated. Deglaciation related meltwater that drives an increase of sea level is held fixed to the default history.
II	The response to variations in the timing of reduction of the background anomaly in freshwater flux applied to the North Atlantic is investigated. The amplitude of the initial background anomaly is held constant and the history of deglaciation related meltwater is held fixed to the default history.
III	This simulation includes the impact upon the variation of surface temperature due to the variation of surface albedo associated with the presence of ICE-4G ice-sheets.

over-freshening of the high-latitude North Atlantic. In our previous analysis using the ocean-only version of the model (Sakai and Peltier, 1996), the annual cycle of SSAT was fixed so that surface cooling did not occur even when heat release from the ocean to the atmospher was reduced. In the coupled version of the model, the cooling caused by the atmosphere-ocean interaction changes the region of intense NADW formation by shifting it southward where the salinity is higher. This process tends to keep the rate of NADW production high, thus reducing the duration of the low-NADW production event (the simulated Y-D).

On the basis of this result we are led to make two important inferences. One is that in the absence of a background component of the freshwater forcing there should be no transition in the intensity of NADW production following LGM but prior to the Y-D. Based upon Fig. 1 which reveals an intense B/A event, the results of this simulation are therefore in conflict with the observations.

The rather poor reproduction of the Y-D event revealed on the top plate of Fig. 5 is clearly improved by increasing the initial background anomaly (which is unrelated to sea level) from zero. This is especially evident in the third plate of Fig. 5. For this balance of contributions to the net freshwater forcing, we obtain both low-NADW-formation and high-NADW-formation states that precede the simulated Y-D. In the 1 kyr period prior to the Y-D, a state of high-NADW-formation develops for background forcing amplitude between 8.33 and 9.52×10^{12} m^3/yr. This feature is very similar to the B/A warm period revealed by the isotopic data shown on Fig. 1. The first of the time series in this sequence reveals a further interesting feature, namely a state of increased simulated NADW production that occurs at the beginning of the record. This feature corresponds to one of the D-O oscillations that we have investigated in our previous work (Sakai and Peltier, 1997): within a certain range of persistent background anomalous forcing, such as that employed in the present study, D-O oscillations are expected to appear. Although this feature is interesting in itself, the Greenland climate record does not exhibit prominent D-O-like oscillations near LGM. According to our simple model, then, the actual anomalous freshwater forcing during deglaciation may have been closer to those assumed in the fourth and fifth plates from the top in Fig. 5. In these two cases, NADW formation is turned off until approximately 14 kyrBP when, following its sudden onset, a state of high-NADW-formation is simulated to persist until onset of the low-NADW-formation state, which constitutes the Y-D, a highly similar sequence to the data shown on Fig. 1. This theory therefore provides the first successful simulation of the B/A event.

The bottom plate of Fig. 5 shows that, with this strength of applied background forcing, a state of negligible NADW activity persists until approximately 12 kyrBP, the time of termination of the actual Y-D. In this extreme case, application of an overly large background anomaly does not allow the NADW formation process to recover at all prior to the Y-D. Again, according to analyses of a variety of paleorecords it is well established that NADW formation did recover to its present intensity sometime between LGM and the Y-D, so that the range of parameter values employed in this simulation is also excluded observationally.

An equally important and more diagnostically direct quantity delivered by the ocean component of the model is the heat flux across the ocean surface, especially near the region where deep convection occurs. Figure 6 shows a corresponding time series from the same set of experiments. In this figure, we show time series of the heat exchange across the surface of the North Atlantic integrated between 30°N and 80°N. Clearly, there exists a very good correlation between the previously discussed proxy for the intensity of NADW formation and the magnitude of heat exchange across the air-sea interface. More intense NADW formation generally results in more intense atmospheric heating.

The influence of such surface heat exchange should also be reflected in the temperature field over

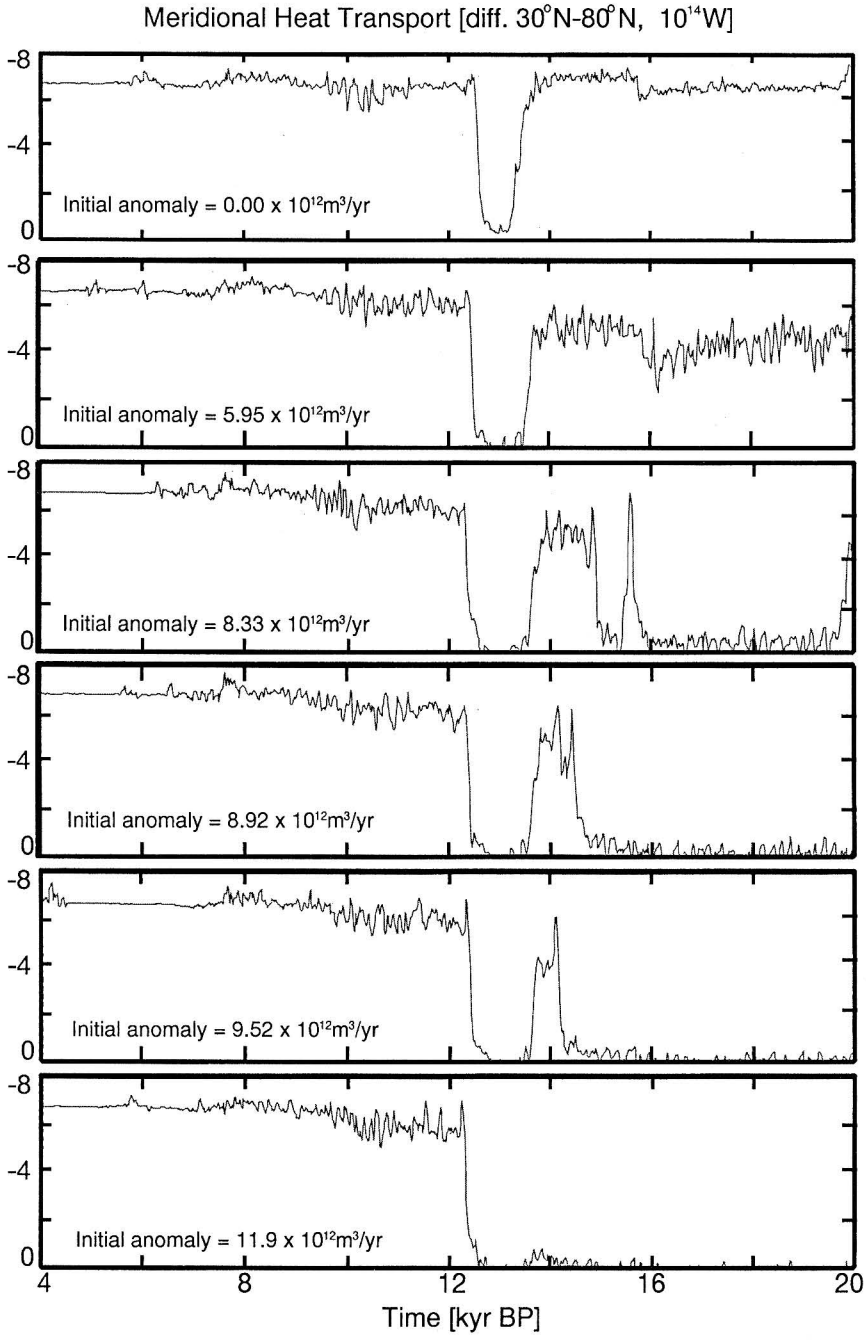

Fig. 5. Results from experiment I. The individual plates present the difference of the meridional heat transport between 30°N and 80°N in the Atlantic Basin for the values of the initial background anomaly depicted on Fig. 3 (since the transport is taken as positive for southward direction, northward heat transport corresponds to the negative sign). The amplitude of this heat transport is proxy for the intensity of NADW.

the Atlantic, and this direct influence is in fact revealed in Fig. 7, in which we have plotted time series of the surface air temperature averaged over the North Atlantic basin of the model between 50°N and 70°N. Since the meridional heat transport is well correlated with the heat exchange across the surface, and the surface heat exchange is well correlated to the temperature field, NADW activity is also well correlated to the temperature field in the same geographical region.

Comparing Fig. 5 with Fig. 7 demonstrates that low-NADW-formation in the North Atlantic results in the creation of a cold climate state over the North Atlantic, and that high-NADW-formation corresponds to a warm state. As mentioned in connection with the model overview, Milankovitch-insolation

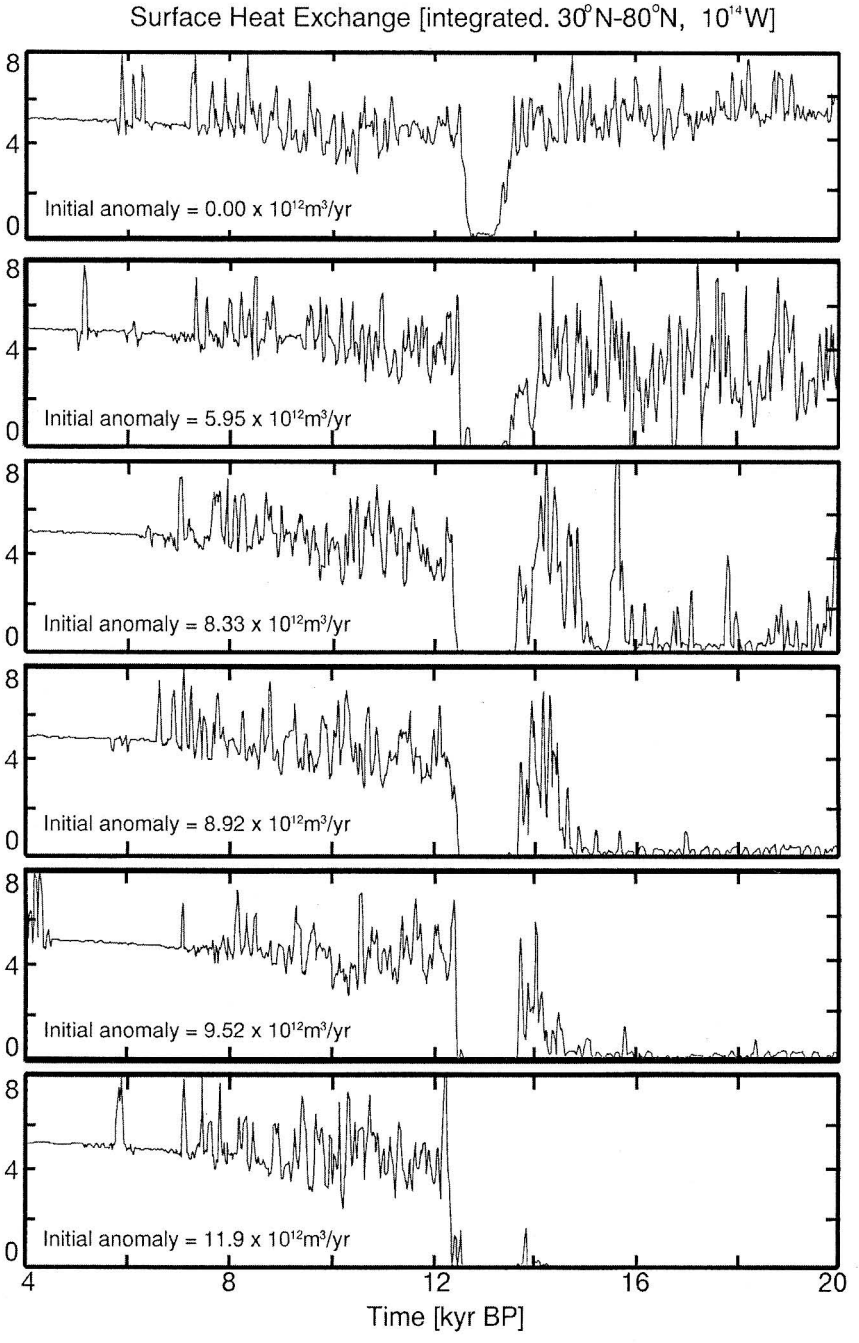

Fig. 6. Results from experiment I. The individual plates present time series of surface heat exchange integrated from 30°N and 80°N over the Atlantic Basin for the same sequence of initial background anomalies as in Fig. 5 (a positive value implies that the ocean is supplying heat to the atmosphere).

forcing has been included in all of the experiments presented herein, but the direct effect of the influence of insolation variations due to the changing geometry of the Earth's orbit (precession, obliquity, eccentricity) is insignificant compared with the influence of the NADW formation process. This is made clear by inspection of the temperature change simulated to occur in connection with the Y-D period. The duration of this cold period is only about 1 kyr, but the insolation change caused by orbital forcing over this period is very small (the shortest of the timescales in the orbital forcing is that of precession, which has a dominant period near 21 kyr). The direct influence of insolation variations may be inferred by comparing temperature near the beginning (near 20 kyrBP) with that near the end (near 4 kyrBP) of the integration, for which results are shown on the top plate of Fig. 7. This yields a variation of approximately 1°C, so that the contribution to the temperature change during deglaciation over

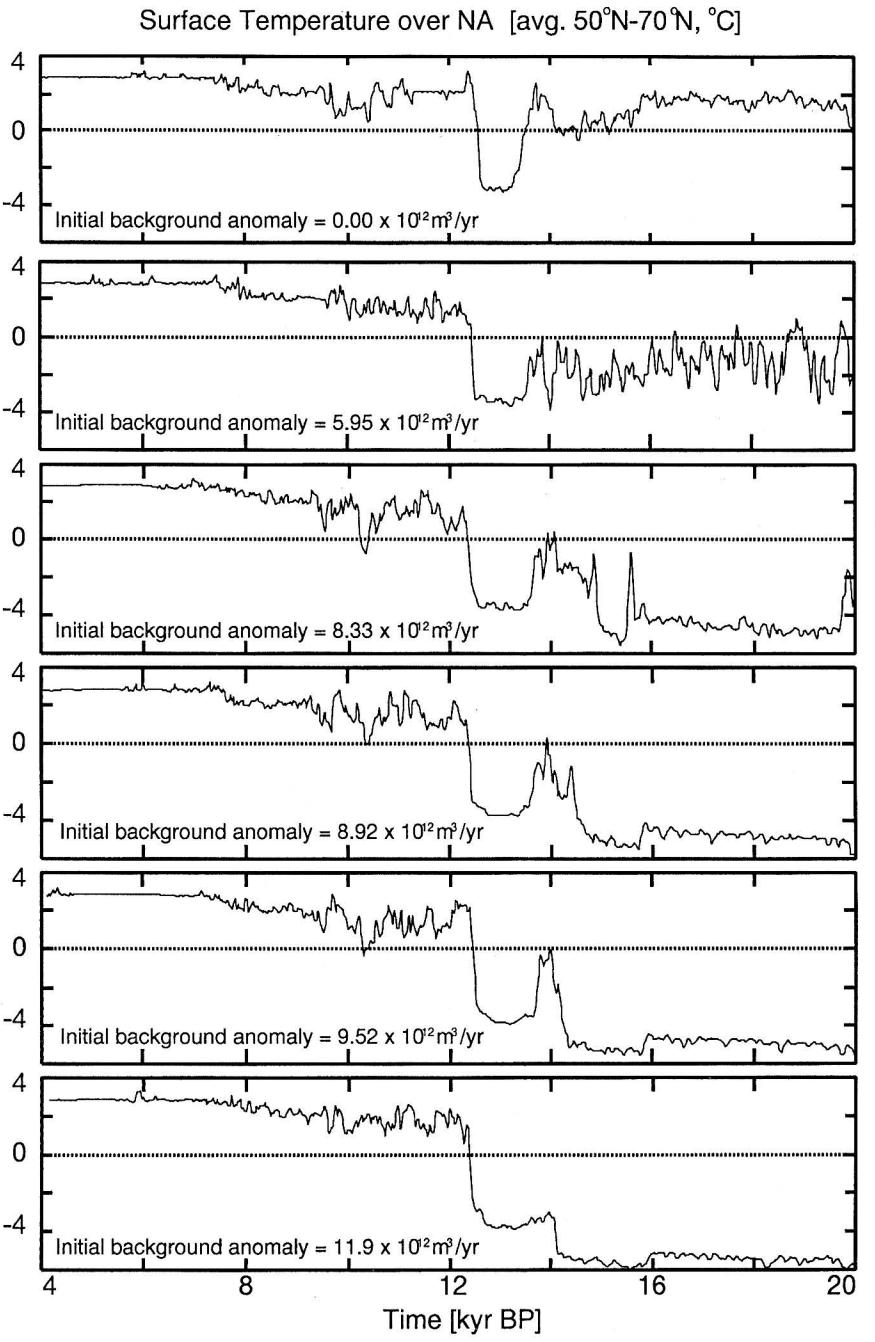

Fig. 7. Results from experiment I. The individual plates present time series of sea surface air temperature averaged between 50°N and 70°N over the Atlantic for the same sequence of initial background components of the freshwater forcing anomaly for which results are shown on Fig. 5.

the high-latitude North Atlantic due to the direct influence of the change in insolation is less than 1°C. On the other hand, the temperature increases that mark the beginning and the end of the Y-D period on Fig. 7 are generally on the order of 6°C. This 6°C amplitude is on the same order as that predicted in our model to occur in conjunction with individual phases of the Dansgaard-Oeschger oscillation (Sakai and Peltier, 1997). It is also in close accord with the observed amplitude of the temperature signal that accompanies both the Y-D and D-O oscillation based upon ice-core derived histories of temperature variations from the Summit, Greenland site.

There is one aspect of these simulated climate histories that shows a slight negative correlation most clearly seen on the top plates of Fig. 5 and Fig. 7. Between 16 kyrBP and 14 kyrBP, NADW formation is still high (slightly higher than that between 18 kyrBP and 16 kyrBP), but the temperature during this period is slightly lower than that between 18 kyrBP and 16 kyrBP. This may be explained as a consequence of the southward migra-

tion of the region of intense NADW formation when temperature decreases over the region. Migration of the position of most intense NADW formation is not necessarily related to the intensity itself. Such migration is, however, inevitable under certain circumstances, namely when the sea surface salinity over the main region of NADW formation decreases for some reason, with sea surface salinity increasing equatorwards. In this circumstance the region will no longer produce NADW and thus cooling will occur. In our EBM-based model, in which horizontal heat transport is diffusive, this cooling propagates quasi-isotropically and this may enable neighboring regions to the south to develop into a new NADW source. In time series generated by averaging over 50°N–70°N, this may simply appear as a decrease in the mean temperature of the region.

The sequence of events that occurs when NADW formation weakens is totally different. Under such conditions, there is no way to release the heat that is stored in North Atlantic deep water (or intermediate water). Although the transport of warm saline water from middle latitudes and summer surface heating in the middle-high latitudes increase the thermal energy of the intermediate layer in the North Atlantic, the low salinity and thus density of the surface water prevents the occurrence of deep convection through which stored thermal energy is released to the atmosphere.

The mechanism that controls the occurrence of the Y-D is, therefore, essentially the same in the coupled model as in the ocean-only model. The new element that is revealed in the simulations that include a background component of the forcing is that the climate model successfully simulates both a Bølling/Allerød warm period and a Younger-Dryas cool period. In Fig. 7, the third to fifth plates suggest cold climate to persist over the North Atlantic prior to the onset of abrupt warming after 15 kyrBP. The cold state otherwise persists essentially from the beginning of the model integration. This structure is in very close accord with the sequence of events that is observed to have occurred between LGM and the onset of the B/A. At the onset of this warm period, the temperature increases abruptly by approximately 4°C as is observed to be characteristic of the onset of B/A. The warm period simulated herein ends near 13.5 kyrBP, which makes the beginning of *Younger-Dryas* cool period in the simulated climate history. This cold state persists in the model until approximately 12 kyrBP, and is the model simulated Y-D. It should be recognized that in this simulation the Y-D occurs somewhat earlier than what is revealed in the observational data shown in Fig. 1.

An important point concerning the stability of the simulated Y-D episode involves the extent to which the duration of this event is modified by the magnitude of the background component of the anomalous freshwater forcing. In the top plate of Fig. 7, the *Y-D* cool period lasts less than 1 kyr. On the fourth and fifth plates, the corresponding *Y-D* periods are stretched so as to reach 1.2–1.4 kyr and thus to agree with the observed duration of the Y-D according to the Summit ice-core isotopic data shown in Fig. 1.

4.2 Timing of the reduction of the background component of the freshwater anomaly flux: exp. II

Since the hypothesis that glacial conditions themselves resulted in the addition of an background anomaly in freshwater flux (unrelated to sea level) being applied to the North Atlantic has some attendant uncertainty, the amplitude of the background anomaly may not be precisely proportional to continental ice cover. This set of experiments is therefore intended to examine the sensitivity of the simulated climate changes during deglaciation to the timing of this component of the anomalous forcing.

Figure 8 shows time series for the variations of meridional heat transport (difference between 30°N and 80°N) in the Atlantic from this set of experiments. Similarly, in Fig. 9 and Fig. 10 are respectively plotted the heat exchange time series across the surface of the Atlantic integrated from 30°N to 80°N and the temperature time series averaged between 50°N and 70°N. The middle plate on each of Figs. 8–10 corresponds to the case of the default deglaciation history of Figure 2, and the upper plates present results obtained when the reduction of the background anomaly proceeds earlier than in the default history, whereas the lower plates present results obtained when the reduction of the background anomaly proceeds later than in the default history. The amplitude of the IBA is of course kept fixed in all of these experiments.

Inspection of those figures demonstrates that when the reduction of the background anomaly is assumed to have begun earlier than in the default case, this leads to the simulation of a longer warm period prior to the Y-D cold period. On the other hand, if the reduction starts later than in the default deglaciation history, the warm period that precedes the Y-D contracts or vanishes entirely.

According to these experiments, a deglaciation scenario after LGM may be described as follows: the deglaciation process at first proceeded slowly, for according to our theory there is no reason for any sudden warming that is caused by a sudden onset of NADW formation to occur. Influenced primarily by a weak change in insolation, surface temperature rises moderately. This slow phase of deglaciation results in a gradual reduction of the anomalous background hydrological perturbation applied to the North Atlantic. Once the background anomaly has been reduced to subcritical amplitude, a sudden recovery of intense NADW formation occurs, which immediately warms the surrounding region

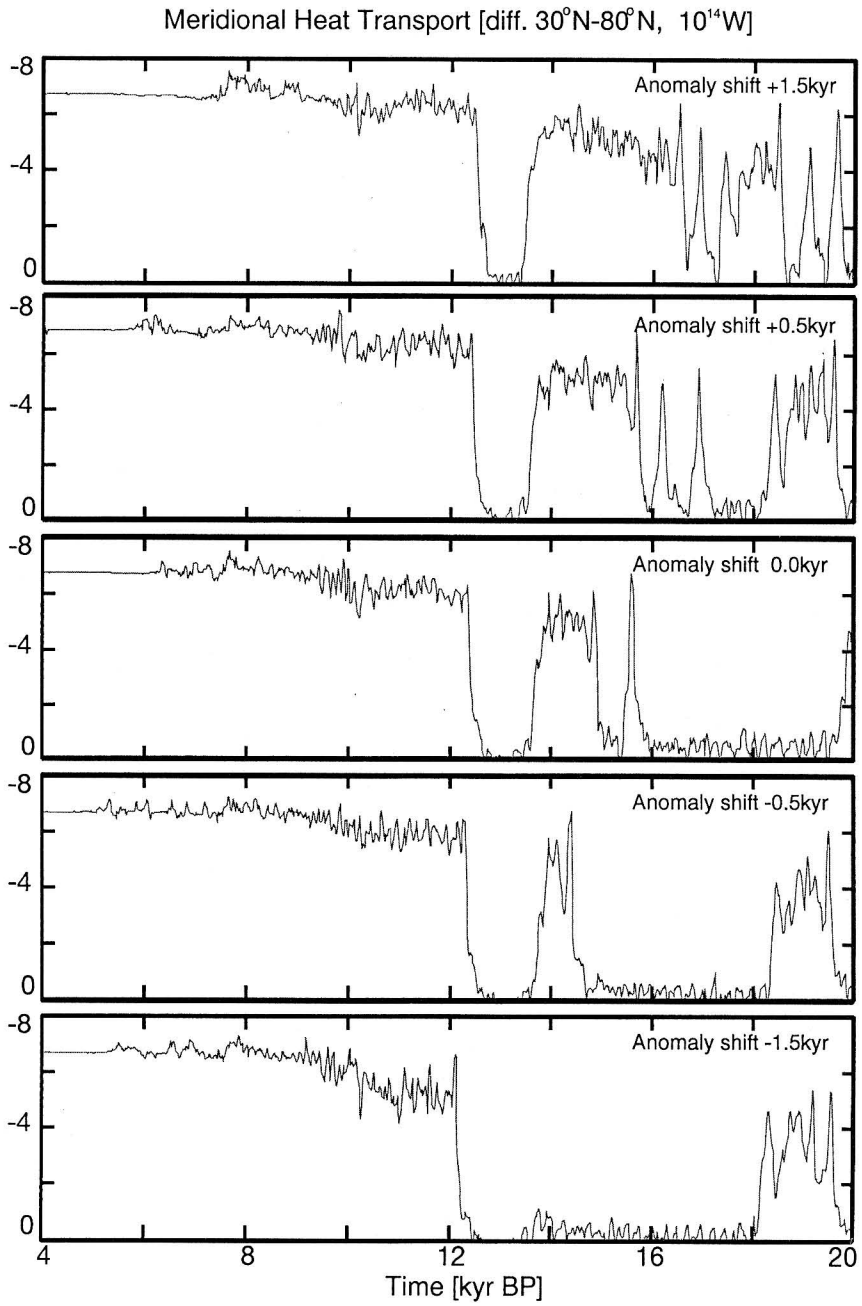

Fig. 8. Results from experiment II. Same as for Fig. 5 except that the time series of meridional heat transport are shown for various assumptions of the timing of the reduction of the background component of the freshwater flux anomaly.

as demonstrated in this and in the preceding subsection. This event corresponds to the onset of the B/A warm period. The B/A period ends with the onset of the Y-D period, which itself results from the freshwater forcing associated with the first intense meltwater pulse that is related to sea level change, that called 1A in Fairbanks (1989). The combination of the background anomaly in freshwater forcing and the deglaciation produced meltwater that actually causes sea level to rise maintains the NADW stagnant cold state in the North Atlantic for 1.2–1.4 kyr. The second onset of abrupt warming occurs at the end of the cold period.

Although this scenario is well supported by our analyses, there is at least one difficulty we are unable to resolve at this point. This concerns the timing between the first meltwater pulse (as recorded by the coral-based sea-level record from Barbados) and the onset of the Y-D. Broecker *et al.* (1989) hypothesized a switching of the location of the applied meltwater load from the Mississippi outlet to St. Lawrence River outlet, which could lead to a more direct application of the meltwater onto the region of NADW formation, and that this more *di-*

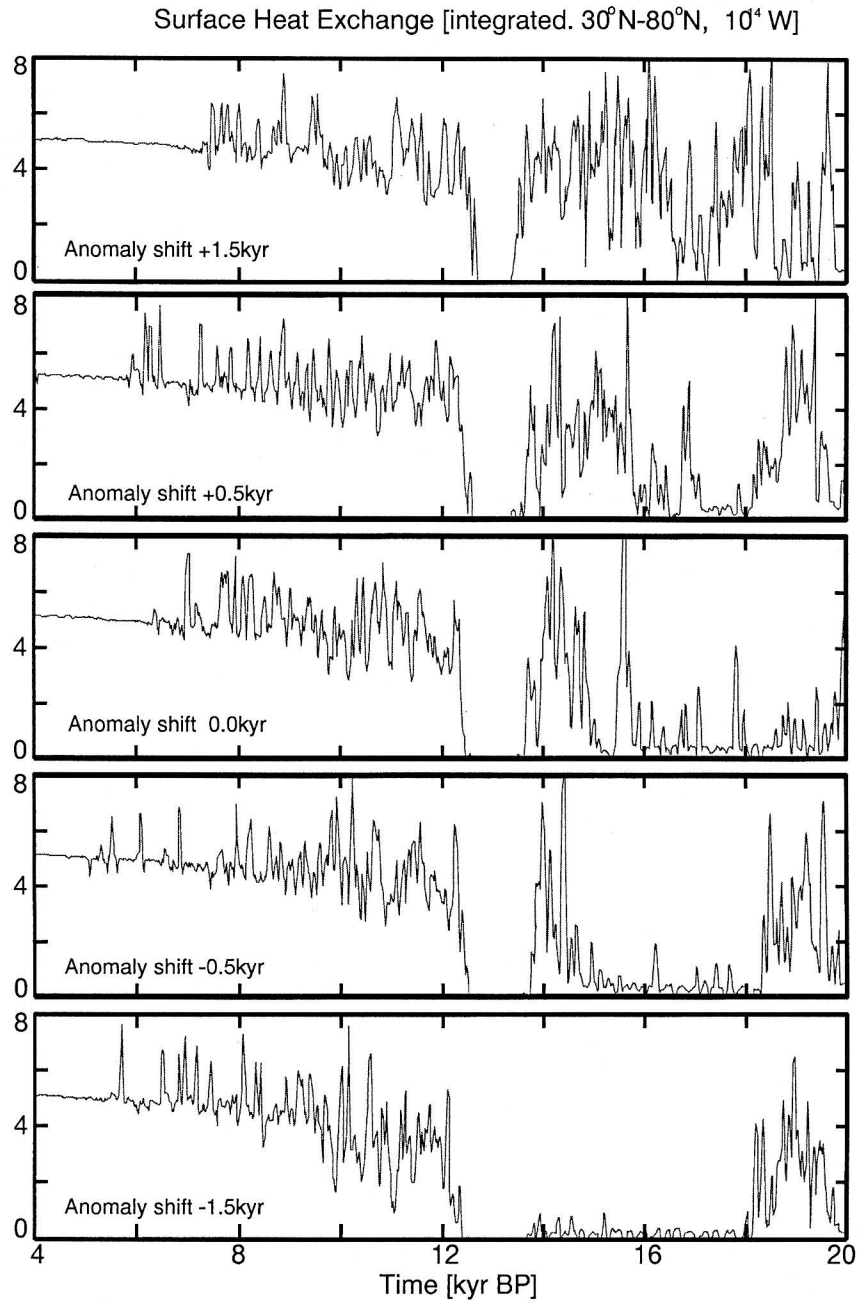

Fig. 9. Results from experiment II. Same as for Fig. 6 except that the time series of heat exchange between the North Atlantic Ocean and the atmosphere are shown for various assumptions concerning the timing of the reduction of the background component of the freshwater anomaly.

rect hit may have been responsible for the onset of the Y-D. In this paper we are obliged to leave this question open since the dimensionality of our model does not allow us to address the issue.

5. Conclusions

A previously constructed two-dimensional model of the global thermohaline circulation, which has already delivered a successful simulation of Dansgaard-Oeschger oscillations (Sakai and Peltier, 1997), has been herein applied to the development of a more complete understanding of the sequence of climate variations that occurred during the last deglaciation event of the current ice-age cycle. The meltwater histories employed for the purpose of the simulations described herein have been based upon the assumption that such history must be composed of two distinct (anomalous) components. One of these is assumed to be that which has a direct expression in eustatic sea level, whereas the second is assumed to have no impact on sea level and so to represent a change of the global hydrological balance that characterizes the modern climate system. Three different primary series of experiments were

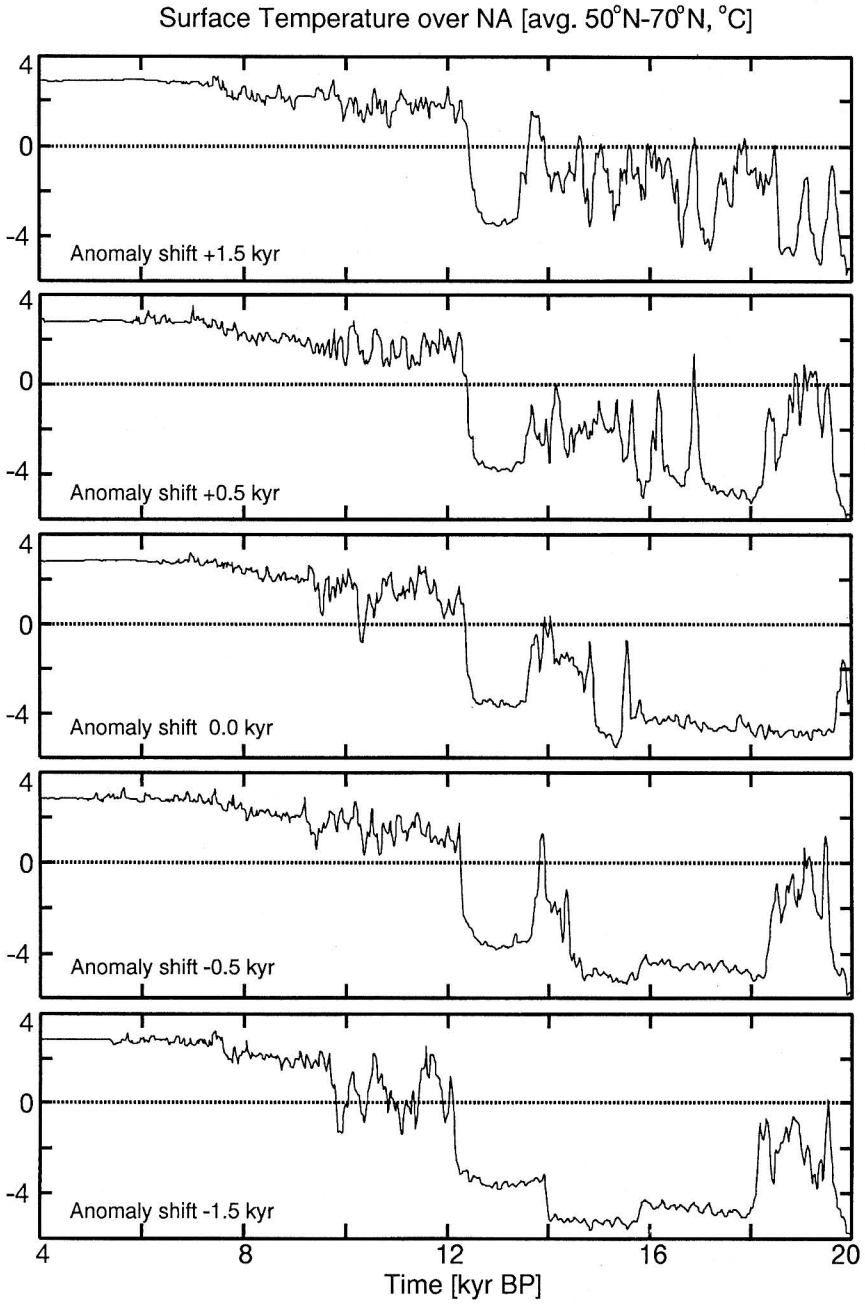

Fig. 10. Results from experiment II. Same as for Fig. 7 except that the time series of sea surface air temperature are shown as a function of the timing of the reduction of the background component of the freshwater flux anomaly.

performed in order to examine the sensitivity of the system to variations in the hydrological forcing of the oceans. Our goal in these analyses was to demonstrate that the complete sequence of climate events that occurred subsequent to LGM, including both the Bølling/Allerød warm period and the Younger-Dryas cool period, might be explained as a consequence of a single hydrological scenario. Insofar as we are aware, our results represent the first successful simulation that has been proposed for the Bølling/Allerød episode.

Appendix

The influence of surface albedo variation due to ICE-4G ice-sheets

It might be interesting to briefly describe a final attempt to simulate the detailed sequence of climate variations that is observed to have occurred during the most recent episode of deglaciation. This experiment may be somewhat *ad hoc*, but we believe it to constitute our best effort to predict a complete deglaciation history with the climate model

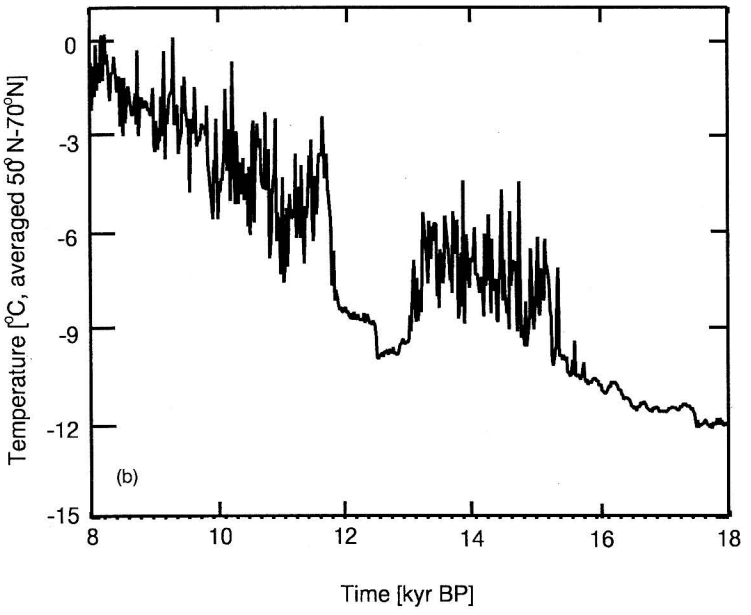

Fig. 11. Results from experiment III, a "best" simulation incorporating the standard meltwater history with the background and sea level related components as well as the influence of surface albedo variations due to the presence of the continental ice-sheets as represented in the ICE-4G model of Peltier (1994).

that employs only an EBM to diagnose temperature and a two-dimensional ocean model to predict oceanic heat flux. In addition to the previously described ingredients in the main part of the paper, in this experiment the model will also include the direct influence of continental ice cover, not based upon the prognostic cryospheric component of the model but rather based upon the ICE-4G model inferred by Peltier (1994, 1996). Since this analysis provides the distribution of surface ice cover only with a time resolution of 1 kyr, the model ice-field is updated only every 1 kyr in the runs of the climate model to be described as follows.

Figure 11 shows the predictions from the climate model, which now includes the direct effect of the surface albedo variation due to the presence of the decaying ice-sheets. One of the most prominent features of the simulated history of surface temperature change is the increased temperature difference between the pre-B/A period and the post Y-D period from that predicted by the previous analyses in this paper. This is apparently induced by the direct influence of the continental ice-sheets, which decreases in area coverage monotonously with time during deglaciation according to the ICE-4G reconstruction. Clearly the surface temperature at a given latitude in this experiment will be much colder than in the previous two sets of experiments. Since the atmospheric EBM contains seasonal feedback associated with snow/sea ice, the colder climate than was obtained previously is caused in part by the increase in surface albedo due to increase of snow/sea ice cover.

The amplitude of the temperature differences simulated for the transition events in this more fully articulated version of the model, *i.e.* the onset of B/A, and the termination of Y-D, agree very well now with inferences based upon the Summit proxy data. There is, however, one clear difference between these model results and the climate proxy records (Fig. 1). Although temperature during the Y-D cool period in the observed climate record is indicated to be as low as during the pre-B/A level, the model prediction suggests that the Y-D temperatures near Greenland were significantly (approximately 2°C) warmer than those characteristic of the pre-B/A level. In the experiments described in preceding subsections, in which no direct influence of continental ice-cover was taken into account, the corresponding temperature difference was found to be less than 2°C. Given the difference in the details of the experiments, this enhancement in the general warming will be understood to be associated with the slow reduction of continental ice cover, which occurs during deglaciation. In spite of the good fit to the observed history of surface temperature variations achieved in this experiment, however, the problem of the timing of the Y-D and B/A events relative to the periods of peak freshwater discharge still remains.

References

Bard, E., B. Hamelin, R.G. Fairbanks and A. Zindler, 1990: Calibration of the ^{14}C timescale over the past

30,000 years using mass spectrometric U-Th ages from Barbados corals. *Nature*, **345**, 405–410.

Bard, E., B. Hamelin, M. Arnold, L. Montagioni, G. Cabioch, G. Faure and F. Rougerie, 1996: Deglacial sea-level record from Tahiti corals and the timing of global meltwater discharge. *Nature*, **382**, 241–244.

Broecker, W.S., J.P. Kennet, B.P. Flower, J.T. Teller, S. Trumbore, G. Bonani and W. Wolfli, 1989: Routing of meltwater from the Laurentide ice sheet during the Younger Dryas cold episode. *Nature*, **341**, 318–321.

Dansgaard, W., S.J. Johnsen, H.B. Clauson, D. Dahl-Jensen, N.S. Gundestrup, C.U. Hammer, C.S. Hvidberg, J.P. Steffensen, A.E. Sveinbjornsdottir, J. Jouzel and G. Bond, 1993: Evidence for general instability in past climate from a 250-kyr ice-core record. *Nature*, **364**, 218–220.

Deblonde, G. and W.R. Peltier, 1993: Pleistocene ice age scenarios based upon observational evidence. *J. Climate*, **6**, 709–727.

Duplessy, J.-C., L. Labeyrie, A. Juillet-Leclerc, F. Maitre, J. Dupart and M. Sarnthein, 1991: Surface salinity reconstruction of the North Atlantic Ocean during the last glacial maximum/*Oceanologica acta*, **14**, 311–323.

Edwards, R.L., J.W. Beck, G.S. Burr, D.J. Donahue, J.M.A. Chappell, A.L. Bloom, E.R.M. Druffel and F.W. Taylor, 1993: A large drop in atmospheric $^{14}C/^{12}C$ and reduced melting in the Younger Dryas, documented with ^{230}Th ages of corals. *Science*, **260**, 962–968.

Fairbanks, R.G., 1989: A 17,000-year glacio-eustatic sea level record: influence of glacial melting rates on the Younger-Dryas event and deep-ocean circulation. *Nature*, **342**, 637–642.

Fairbanks, R.G., 1990: The age and origin of the "Younger Dryas climate event" in Greenland ice cores. *Paleoceanogr.*, **5**, 937–948.

GISP2, 1993: The 'flicking switch' of late Pleistocene climate change. *Nature*, **361**, 432–436.

GRIP, 1993: Climate instability during the last interglacial period recorded in the GRIP ice core. *Nature*, **364**, 203–207.

Grootes, P.M., M. Stuiver, J.W.C. White, S. Johnsen and J. Jouzel, 1993: Comparison of oxygen isotope records from GISP2 and GRIP Greenland ice cores. *Nature*, **366**, 552–554.

Jouzel, J., C. Lorius, J.R. Petit, C. Genthon, N.I. Barkov, V.M. Kotlyakov and V.M. Petrov, 1987: Vostok ice core: A continuous isotope temperature record over the last climatic cycle (160,000 years). *Nature*, **329**, 403–408.

Kennett, J.P. and B.L. Ingram, 1995: A 20,000-year record of ocean circulation and climate change from the Santa Barbara basin. *Nature*, **377**, 510–514.

Meese, D., R. Alley, T. Gow, P.M. Grootes, P. Mayewski, M. Ram, K. Taylor, E. Waddington and G. Zielinski, 1994: *Preliminary depth-age scale of the GISP2 ice core. Special Report 94-1*, CRREL.

Peltier, W.R., 1994: Ice age paleotopography. *Science*, **265**, 195–201.

Peltier, W.R., 1996: Mantle viscosity and ice-age ice topography. *Science*, **273**, 1359–1364.

Sakai, K. and W.R. Peltier, 1995: A simple model of the Atlantic thermohaline circulation: internal and forced variability with paleoclimatological implications. *J. Geophys. Res. -Oceans*, **100**, 13455–13479.

Sakai, K. and W.R. Peltier, 1996: A multi-basin reduced model of the global thermohaline circulation: paleoceanographic analyses of the origins of ice-age climate variability. *J. Geophys. Res. -Oceans*, **101**, 22535–22562.

Sakai, K. and W.R. Peltier, 1997: Dansgaard-Oeschger oscillations in a coupled atmosphere-ocean climate model. *J. Climate*, **10**, 949–970.

Tarasov, L. and W.R. Peltier, 1997: Terminating the 100 kyr Ice-Age Cycle. *J.Geophys.Res.-Atmospheres*, (submitted.)

Taylor, K.C., G.W. Lamorey, G.A. Doyle, R.B. Alley, P.M. Grootes, P.A. Mayewski, J.W.C. White and L.K. Barlow, 1993: The 'flickering switch' of late Pleistocene climate change. *Nature*, **361**, 432–436.

解氷にともなう気候変動：Bølling/Allerød 温暖期及び Younger-Dryas 寒冷期を再現する氷期から間氷期への気候遷移のモデル実験

酒井孝太郎
（名古屋大学大気水圏科学研究所）
W. Richard Peltier
（カナダ・トロント大学大気物理科）

気候システムの長期変動特性を調べるために、以前より開発されてきた二次元多海洋全球熱塩循環モデルをエネルギー収支大気モデルに非同期結合させた。当結合モデルはグリーンランド氷床のサミットコアによって明らかにされた Dansgaard-Oeschger 気候振動のシミュレーションを既に行なったが、今回は最終氷期以降の解氷期間中、一時的な大陸氷床融解水に対する気候システムの応答を調べた。モデルに対しては二つの水循環に関する強制を加えた。一つは珊瑚礁記録に基づいた最終氷期最大期以降の海水準変動に関係する部分で、もう一つは海水準変動とは無関係に現在深層水が生成される北大西洋を囲むように存在した大陸氷床に起因する部分として仮定されるものである。結果として、千年程度の Younger-Dryas に類似の寒冷期以降の海水準変動に伴う融解水の与え方にあまり依存せず、当モデルは Younger-Dryas に類似の寒冷期を再現した。しかし、Younger-Dryas に先立つ Bølling/Allerød 温暖期を当モデルで説明するためには更にバックグラウンド的に北大西洋に海水準変動と関係しない淡水供給を付加する事が必要である事が示された。本研究ではこれら二種類の淡水供給に関する摂動に対する気候の応答の感度も調べている。